Rate 2/3 modulation code for suppression of intrachannel nonlinear effects in high-speed optical transmission

I.B. Djordjevic, B. Vasic and V.S. Rao

Abstract: An efficient approach in suppressing of intrachannel nonlinear effects using modulation codes is proposed. Significant Q-factor improvement ranging from 7–13 dB depending on modulation format, extinction ratio and number of spans is demonstrated. The encoder design is described, and sliding window decoding logic is given.

1 Introduction

RZ high speed transmission over long-haul dispersion-managed links is severely limited by intrachannel nonlinear effects [1–8], such as intrachannel four-wave mixing (IFWM) and intrachannel cross-phase modulation (IXPM). In IXPM, neighbouring pulses interact as they overlap during transmission causing a frequency shift in each other. The frequency shift is dependent on the pulse pattern and in turn causes timing jitter. In IFWM, at sufficiently high dispersion, energy is transferred to the middle of a neighbouring bit slot [2] causing either a ghost (spurious) pulse if the bit slot is empty or amplitude jitter in a non-empty bit slot. Since the energy-growth of a ghost pulse is proportional to the distance-squared (in loss-less fibre) [3] the 'ghost' pulses gain sufficient energy to be detected as '1's by the detector at the output of the channel resulting in transmission error.

Common approaches employed to tackle IFWM are to remove phase coherence between neighbouring pulses [2, 4], to randomise phase completely or to employ alternate polarisation modulation formats [5].

A rather different approach for reducing the occurrence of ghost pulses is proposed in this paper, namely modulation coding (line coding or constrained coding) [9]. The modulation code adds redundancy which is used to correctly decode transmitted data, and reduces the occurrence of ghost pulses by avoiding bit patterns causing the effect. More specifically, we propose a rate 2/3 modulation code imposing a constraint on the occurrence of 'resonant' pulse triples contributing the most to the creation of ghost pulses. The encoder design and sliding window decoder logic are described in Section 3. Simplicity of encoder and decoder suggest the possibility for all-optical realisation, the property important for applications higher than 40 Gb/s like 160 Gb/s applications. Significant performance improvement is obtained by implementing the proposed approach as demonstrated in the numerical results section.

IEE Proceedings online no. 20050014

doi:10.1049/ip-opt:20050014

Paper first received 3rd February and in final revised form 27th May 2005

The authors are with Department of Electrical and Computer Engineering, University of Arizona, Tuscon, AZ, 85721, USA

E-mail: ivan@ece.arizona.edu

2 Intrachannel nonlinear effects

The signal propagation through the transmission medium is modelled by the generalised nonlinear Schrödinger equation (GNLSE) [10, 11],

$$\frac{\partial A}{\partial z} = -\frac{\alpha}{2}A - \frac{i}{2}\beta_2\frac{\partial^2 A}{\partial T^2} + \frac{\beta_3}{6}\frac{\partial^3 A}{\partial T^3} + i\gamma\left(|A|^2 - T_R\frac{\partial |A|^2}{\partial T}\right)A \quad (1)$$

where z is the propagation distance along the fibre, relative time $T = t - z/v_g$ gives a frame of reference moving at the group velocity v_g, $A(z, T)$ is the complex field amplitude of the pulse, α is the attenuation coefficient of the fibre, β_2 is the group velocity dispersion (GVD) coefficient, β_3 is the second-order GVD, γ is the nonlinearity coefficient giving rise to Kerr effect nonlinearities: self-phase modulation (SPM), cross-phase modulation (XPM) and four-wave mixing (FWM) and T_R is the Raman coefficient describing the stimulated Raman scattering (SRS).

In high-speed transmission, at 40 Gb/s and above, the most important fibre nonlinearities are intrachannel nonlinearities: SPM, IXPM and IFWM. To study the interactions among the pulses within the channel, the field of a single channel can be decomposed as a sum of fields of individual pulses

$$A = \sum_{l=1}^{L} A_l$$

where A_l represents the lth pulse (out of L) centred at $t = t_l$. GNLSE can be rewritten, after the substitution, as

$$\sum_{l=1}^{L}\left(\frac{\partial A_l}{\partial z} + \frac{\alpha}{2}A_l + \frac{i}{2}\beta_2\frac{\partial^2 A_l}{\partial T^2} - \frac{\beta_3}{6}\frac{\partial^3 A_l}{\partial T^3}\right) = i\gamma\sum_{l,k,m=1}^{L} A_l A_k A_m^* \quad (2)$$

(SRS term was ignored to keep the explanation simpler.) The intrachannel nonlinearities may be identified as follows. The case $l = k = m$ corresponds to SPM, the case

$l \neq k \neq m$ or $l = k \neq m$ to IFWM, and the case $l = m \neq k$ or $k = m \neq l$ to IXPM.

2.1 Intrachannel four-wave mixing

In dispersion-managed systems pulses undergo periodical widening and compression as they travel during transmission. The strongest interaction is at the point at which the pulses partially overlap, and to keep the IXPM low in pseudo-linear transmission, the pulses are allowed spread over many bit-periods. However, in the pseudo-linear regime the second intrachannel nonlinear effect-IFWM occurs [1–5], which result in energy transfer among the pulses within the same wavelength channel; resulting in amplitude jitter if energy is transferred in a nonempty bit-slot or in ghost pulse creation if the energy is transferred in an empty bit-slot, as illustrated in Fig. 1. The pulses at positions k, l and m, according to (2) may create a ghost pulse in an empty bit-slot located at $m + k - l$ ('the resonant condition'). Avoiding all such triples is not realistic, since the rate of corresponding constrained code tends to zero. The challenge is to simultaneously minimise both IXPM and IFWM.

2.2 Tackling nonlinearities

Various modulation formats have been proposed to tackle the effects of nonlinearities [2]. As the creation of ghost pulses is a phase sensitive effect, these solutions aim to reduce ghost pulses by removing phase coherence in the pulses, emitted by the optical transmitter, in a given neighbourhood. In another proposed format [4], the phase of local pairs of '1's that surround a '0' are made to be opposite. This may be achieved by switching phase of consecutive '1's or by switching phase of groups of '1's that surround a '0'. In another approach, recently reported [5], the polarisation of adjacent pulses was changed so that they are orthogonal to each other.

In this work, we propose an alternative method for reducing the occurrence of ghost pulses based on line coding. It can be shown that any modulation format may be viewed as a trivial line code with a memory of one and rate one (see [9] for more details). By using a modulation code we can work around the limitations of the channel without significantly increasing the complexity of the system. The line code used thus reduces the occurrence of ghost pulses by avoiding bit patterns that cause the effect.

3 Modulation codes

In the previous Sections we have identified certain bit triples that cause extensive IFWM giving rise to ghost pulses. The optical system can therefore be viewed as a constrained system [9]. The role of a line code (also called modulation codes or constrained codes [9]) is to impose certain constraints on a transmitted sequence to avoid those waveforms that are most likely to be incorrectly received. A modulation encoder translates an arbitrary user bit stream into a bit stream that satisfies the constraints of the channel. For the price of some reduction in user bandwidth and increase in encoder complexity the channel BER is improved as the code works around the constraint that was causing errors in the transmitted bits.

Our goal is to design a code which avoids the patterns that cause the most distortion in pulses transmitted over an optical channel. To do this, we draw directed graph models of constraints that represent the allowed sequences and then design codes based on these graphs. Our code construction is based on a constrained system theory from [9] (the rest of this section uses the terminology from [9]). Many different constraints were considered and a reasonable choice of code was made after studying the graphs. As previously mentioned, triples of pulses interact to cause ghost pulses. The closer the triples are in time, the stronger their interaction. The code we use is designed to avoid three or more consecutive '1's. By doing so, we avoid the worst of the triples. Our code further avoids the resonance patterns '1101', '1011' and '11011'. The directed graph model of such a system is depicted in Fig. 2. Notice that this constraint is similar to the maximum transition run (MTR) constraint proposed for data storage systems [7], but that in addition to forbidding 111 (as in MTR code), our constraint forbids the double resonance pattern '11011'. Valid sequences can be obtained by reading off the edge labels while making transitions from one state to another according to orientation of the edges. The adjacency matrix for the directed graph shown in Fig. 2 is given by

$$A = \begin{bmatrix} 1 & 1 & 0 & 0 \\ 0 & 0 & 1 & 1 \\ 0 & 0 & 0 & 1 \\ 1 & 0 & 0 & 0 \end{bmatrix}$$

Since the constraint prevents us from using all possible bit sequences, the capacity of a constrained system, which defines the highest code rate possible, will be less than '1'. In fact, it can be shown that the capacity is given by $C = \log_2 \lambda_0$, where λ_0 is the largest eigenvalue of the adjacency matrix. It is determined by solving the characteristic equation $\det(A - \lambda I) = 0$. From Shannon theory and Perron–Frobenius theory [9], it follows that a code of rate $R \leq C$ can be constructed. The code efficiency is defined as $\eta = R/C$. Getting back to constrained system from Fig. 2, using the directed graph codes with rates up to $C = 0.6942$ (largest eigenvalue = 1.618) can be designed. For example, by taking the 10th power of the adjacency matrix, the first element on the main diagonal is found to be 64. Therefore, the block code of rate 0.6 can be designed with these 64 codewords of length 10 bits each. From practical point of view the code of rate 0.66, which encodes two user bits into three code bits, would be easier to implement. The efficiency of this code is $\eta = 96\%$. To design this code,

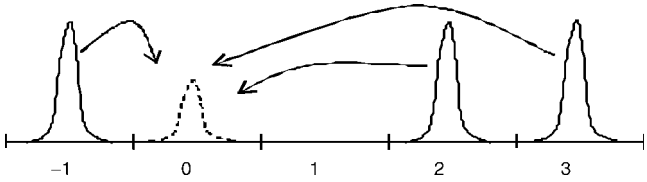

Fig. 1 *Pulses at k, l, m ($k = l + m$)*
Pulses at positions 2, 3 and −1 give rise to a ghost pulse at position 0

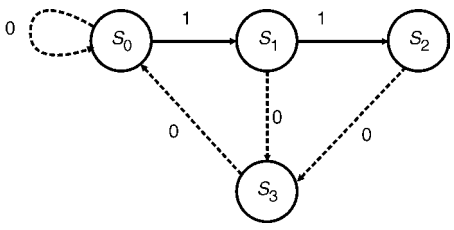

Fig. 2 *Directed graph for given constraint*

a procedure known as the 'state-splitting' algorithm [12] is applied. The procedure starts by taking the third power of the graph from Fig. 2, and the resulting graph is shown in Fig. 3.

The label attached to each branch represents the output pattern for that particular transition. To design a rate 2/3 code, we need to assign two-bit input patterns to each branch. Also, we need $2^2 = 4$ outgoing edges from each state. Checking the states in Fig. 3, we see that State 1 has six outgoing edges, State 2 has three outgoing edges, State 3 has two outgoing edges and State 4 has four outgoing edges. Thus, the rate 2/3 code cannot be designed directly from this graph, and we have to employ the 'state-splitting' algorithm, as follows.

Step 1: Calculate the 'Approximate eigenvector'.

a) Start with an approximation

$$V^{(0)} = (L, L, L, \ldots, L)$$

where L is some positive integer.

b) Compute $V_i^{(k)} = \min(V_i^{(k-1)}, \lfloor (1/2^p) \sum_j a_{ij}^q V_j^{(k-1)} \rfloor)$ $0 < i \leq N$, $0 < j \leq N$ where N is the total number of states, q is the power of the graph, 2^p is the total number of necessary branches leaving each state, and a_{ij} are the elements of the third power of the adjacency matrix A.

c) Repeat step *b*) iteratively till $V_i^{(k)} = V_i^{(k-1)}$, $0 < i \leq N$. $V^{(k)}$ satisfies the relation $A^q V^{(k)} \geq 2^p V^{(k)}$.

The approximate eigenvector for the graph from Fig. 3 is [3 2 1 2]. Since none of the elements is 0, no any state can be excluded from the graph.

Step 2: Assign weights to each branch. The weight of a branch that represents a transition from state S_1 to state S_2 is equal to the approximate eigenvalue V_2 of the sink state S_2.

Step 3: By analysing the states that do not have the necessary number of outgoing edges, select a state to be split. We select S_1 as it has 6 outgoing edges and since splitting it will help states S_2 and S_3 gain more outgoing edges.

Step 4: Given that E_i represents the edges leaving state S_i, the state S_i is split into two states S_{i1} and S_{i2} such that $E_i = E_{i1} \cup E_{i2}$. The edges are split into two groups so that the following equations are satisfied:

$$\sum w(E_{i1}) \geq y_1 2^p \quad \text{and} \quad \sum w(E_{i2}) \geq y_2 2^p$$

Here, $\sum w(E_{i1})$ stands for the sum of the weights of the edges leaving state S_{i1} and $\sum w(E_{i2})$ stands for the sum of the weights of the edges leaving state S_{i2}. y_1 and y_2 are two positive integers that now represent the approximate eigenvalues of states S_{i1} and S_{i2} and, the weight of edges leading to states S_{i1} and S_{i2}.

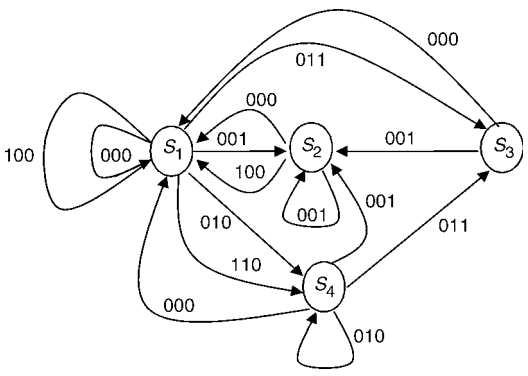

Fig. 3 *Third power of graph in Fig. 2*

The edges leaving state S_1 are split into two groups given by

S_{11}: Branches 000 and 011 ($y_1 = 1$)

S_{12}: Branches 100, 001, 110, 010 ($y_2 = 2$)

The steps of the state-splitting algorithm are repeated till all the states have at least 2^p outgoing edges. To design a 2/3 rate code using the directed graph shown in Fig. 3, states were split in the following order: (i) state S_1 was split into S_{11} and S_{12}, (ii) state S_{12} was split into S_{121} and S_{122}, and (iii) state S_4 was split into S_{41} and S_{42}. This leads to a directed graph with eight states described in Table 1.

The input bits corresponding to each branch are assigned in order to facilitate the construction of the sliding window decoder. Only four outgoing edges are used per state.

The decoder is designed as a sliding window decoder. At maximum, three codewords (nine bits) are used to decode two user bits. Naming the present three bits as ABC, the next six bits as DEFGHI and the previous three bits as XYZ, the sliding window decoder decodes input $I_1 I_2$ corresponding to ABC as

$$\text{If ABC} = \text{“011”}$$
$$I_1 = 0$$
$$I_2 = Y'$$

Table 1: Directed graph for the 2/3 rate code

Previous state	Next state	Input pattern	Branch label
S_{11}	S_{11}	00	000
S_{11}	S_{121}	10	000
S_{11}	S_{122}	11	000
S_{11}	S_3	01	011
S_{121}	S_{21}	01	001
S_{121}	S_{22}	11	001
S_{121}	S_{11}	10	100
S_{121}	S_{122}	–	100
S_{121}	S_{121}	00	100
S_{122}	S_{41}	10	010
S_{122}	S_{42}	01	010
S_{122}	S_{41}	00	110
S_{122}	S_{42}	11	110
S_{21}	S_{11}	00	000
S_{21}	S_{21}	01	001
S_{21}	S_{22}	11	001
S_{21}	S_{11}	10	100
S_{22}	S_{121}	10	000
S_{22}	S_{122}	11	000
S_{22}	S_{121}	00	100
S_{22}	S_{122}	01	100
S_3	S_{121}	10	000
S_3	S_{122}	11	000
S_3	S_{11}	00	000
S_3	S_{21}	01	001
S_3	S_{22}	–	001
S_{41}	S_{11}	00	000
S_{41}	S_{122}	11	000
S_{41}	S_{41}	10	010
S_{41}	S_{42}	01	010
S_{42}	S_{121}	10	000
S_{42}	S_{21}	01	001
S_{42}	S_{22}	11	001
S_{42}	S_3	00	011

For all other patterns of ABC

$$I_2 = C'(B'EF' + BD'F) + E'(A'B'CF'(I' + G') + D'(BC'H'(GI' + G'I) + A'B'CF))$$

and

$$I_1 = I_2(F'(E'HI' + C(H'I + G)) + AB) + C'(A'B'DF' + D'(A(B'F'I_2' + EF) + A'(I_2'(B(I' + G') + E'F) + EF')))$$

4 Numerical results

The simulations were run on a realistic dispersion managed 40 Gb/s channel model. Since our focus is on IFWM and IXPM, the noise generated by the various devices was excluded. We take care of modulation, extinction ratio, realistic models (except for noise) of transmitter, optical filter and electrical filter, ISI, crosstalk effects, Kerr nonlinearities (self-phase modulation, cross-phase modulation, four-wave mixing), and dispersion effects (chromatic dispersion, second order dispersion). For light propagation through the fibre, the nonlinear Schrödinger equation (1) was solved using the split step Fourier method.

The dispersion map [6] is of length $L = 48$ km and consists of $2L/3$ km of D+ fibre followed by $L/3$ km of D− fibre. The fibre parameters are as follows. D+ fibre; dispersion of 20 ps/nm-km, dispersion slope of 0.06 ps/nm^2-km, effective area equal to 110 μm^2 and loss equal to 0.19 dB/km. D− fibre; dispersion of −40 ps/nm-km, dispersion slope of −0.12 ps/nm^2-km, effective area equal to 30 μm^2 and loss equal to 0.25 dB/km. The average dispersion and dispersion slope of the map are zero. The nonlinear Kerr coefficient is 2.6×10^{-20} m^2/W. Linear precompensation and postcompensation are also used. 25 to 60 spans of this map are used to form a channel that is between 1200 km to 2880 km long. The simulations were carried out with an average channel power of 0 dBm with a central wavelength of 1552.524 nm.

The uncoded eyes were generated by passing a 1024 bit long PRBS sequence through the channel and then plotting the eye by overlapping the contents of each bit period. The same sequence was then encoded using our code and the encoded sequence was transmitted through the channel. At the receiver, the eyes were plotted by again overlapping the contents of each bit period. Two different modulation formats–return-to-zero (RZ) and carrier-suppressed return-to-zero (CSRZ) were considered.

Figures 4(*a*–*d*) show the eye diagrams observed for the (4*a*, 4*c*) uncoded and (4*b*, 4*d*) encoded case using RZ format on a 25 span (1200 km) channel. For the simulations depicted in Figs. 4(*a*–*b*), the extinction ratio (power in '1' bit slot/power in '0' bit slot) was set to 13 dB which is common for MZ modulators available at 40 Gb/s. In this case a Q-factor improvement of 6.73 dB was observed.

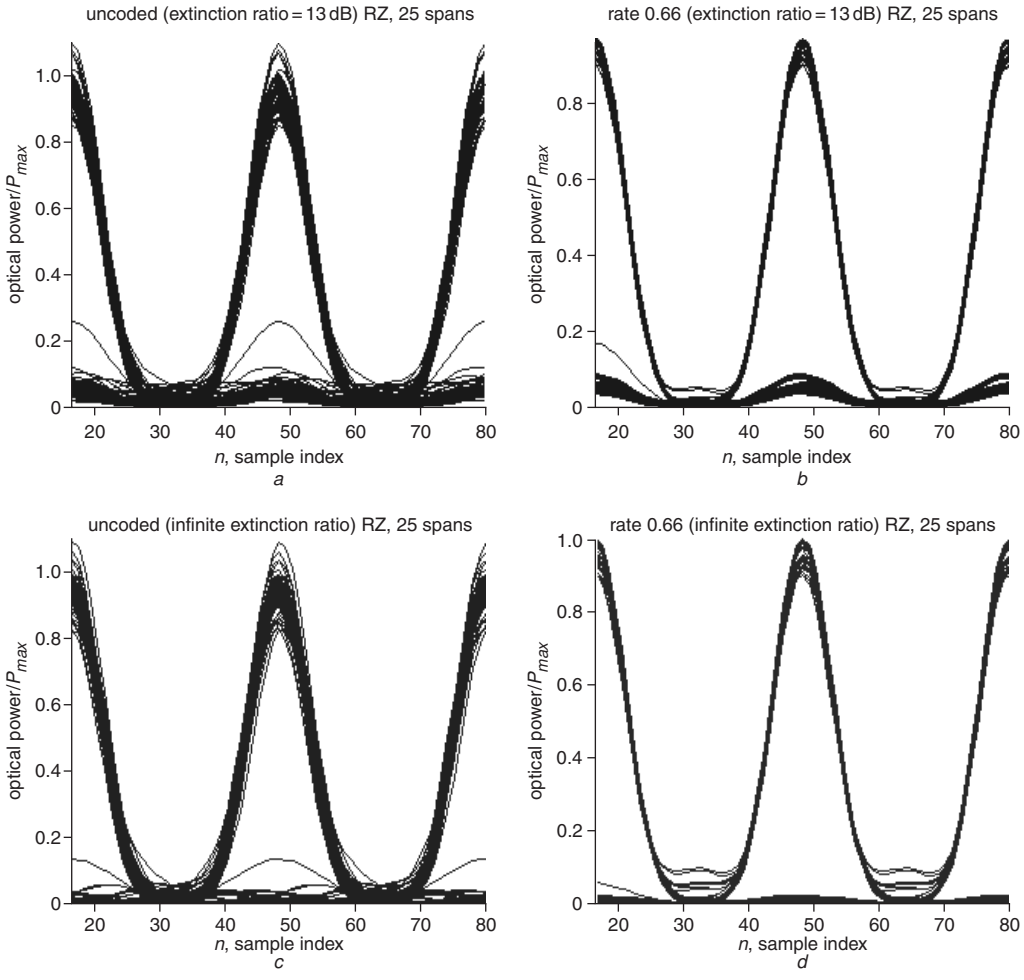

Fig. 4 *Eye diagrams (32 samples per bit) after 1200 km*

Average powers of 0 dBm with a precompensation of −320 ps/nm, zero residual dispersion, RZ format
a Uncoded eye *b* Encoded eye — Extinction ratio of 13 dB
c Uncoded eye *d* Encoded eye — Infinite extinction ratio

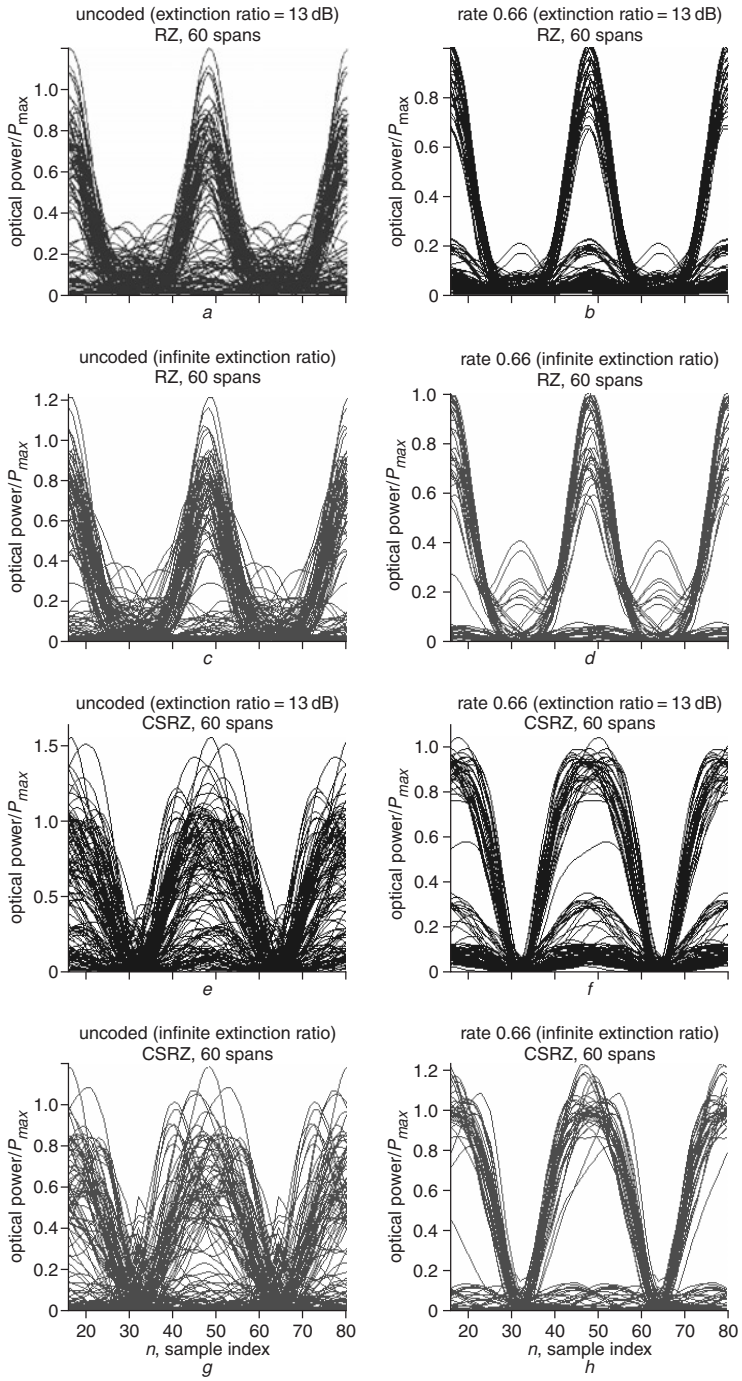

Fig. 5 *Eye diagrams (32 samples per bit) after 2880 km*

Average powers of 0 dBm with a precompensation of −320 ps/nm, zero residual dispersion and extinction ratio of 13 dB.
RZ format:
a Uncoded eye
b Encoded eye — Extinction ratio 13 dB
c Uncoded eye diagram
d Encoded eye diagram — Infinite extinction ratio
CS-RZ format:
e Uncoded
f Encoded case — Extinction ratio 13 dB
g Uncoded eye diagram
h Encoded eye diagram — Infinite extinction ratio

The Q-factor is calculated after optical filtering (of bandwidth 80 GHz), photo-detection and electrical filtering (of bandwidth 26 GHz). Q-factor improvement is defined as

$$20 \log_{10}(Q_{\text{encoded}}(R_b/R)/Q_{\text{uncoded}}(R_b)) \qquad (3)$$

where with R_b is denoted the bit rate and with R the code rate. For the simulations depicted in Figs. 4(*c*–*d*) on the other hand, infinite extinction ratio was used. In this case a Q-factor improvement of 8.45 dB was found. In both cases we see an improvement in amplitude jitter and reduced ghost pulse.

Figures 5(*a*–*d*) show the eye diagrams observed for the uncoded and encoded case using RZ format on a 60 span (2880 km) channel. When the extinction ratio was set to 13 dB (Figs. 5(*a*–*b*)), a Q-factor improvement of 9.49 dB was observed. When the extinction ratio was set to infinity, (Figs. 5(*c*–*d*)), a Q-factor improvement of 9.92 dB was

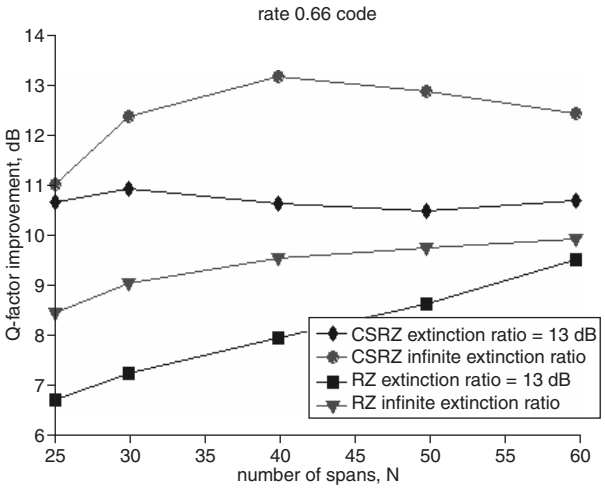

Fig. 6 *Q-factor improvement for different number of spans*

observed. In both cases the uncoded eyes are almost completely closed while in the encoded case the eye diagrams are widely opened. Figs. 5(*e*–*h*) show the eye diagrams observed for the uncoded and encoded case using CS-RZ format on a 60 span (2880 km) channel. When the extinction ratio was set to 13 dB (Figs. 5(*e*–*f*)), a Q-factor improvement of 10.67 dB was observed. For the simulations shown in Figs. 5(*g*–*h*) infinite extinction ratio was used and in this case a Q-factor improvement of 12.41 dB was observed.

Finally, the number of spans is varied between 25 and 60 and the Q-factor improvement achieved is plotted in Fig. 6.

5 Conclusion

We propose the use of modulation codes to counter the effects of IFWM and IXPM in high data-rate channels. A rate 2/3 code based on a constraint that avoids 'resonance' triples of pulses has been presented along with encoder design and sliding window decoder logic. The simplicity of encoder and decoder offers the possibility for both all-optical and electrical implementations. The code successfully counters the detrimental effects of nonlinearities.

Modulation decoder is usually implemented as a Boolean function applied on a finite number of bits surrounding the bit to be decoded. In other words, the decoder can use only hard decision channel outputs and processes hard bits, therefore prohibiting soft iterative decoding. The proposed modulation code can be combined with a RS code as an inner code. It can be also combined with a concatenation of two RS codes. Therefore, it is can be used in conjunction with both the first and the second generation of FEC proposed for long-haul optical transmission [RS(255,239) and RS(255,239) + RS(255,233) concatenation, respectively] [13]. An alternative scheme that circumvents the above mentioned soft decoding problem is known as reverse concatenation, and it has been adopted in our recent paper [14].

6 Acknowledgments

This work was funded in part by the NSF under Grants ITR 0325979 and CCR 0208597.

7 References

1 Essiambre, R.-J., Mikkelsen, B., and Raybon, G.: 'Intra-channel cross-phase modulation and four-wave mixing in high-speed TDM systems', *Electron. Lett.*, 1999, **35**, (18), pp. 1576–1578
2 Forzati, M., Martensson, J., Berntson, A., Djupsjobacka, A., and Johannisson, P.: 'Reduction of intrachannel four-wave mixing using the alternate-phase RZ modulation format', *IEEE Photon. Technol. Lett.*, 2002, **14**, (9), pp. 1285–1287
3 Ablowitz, M.J., and Hirooka, T.: 'Resonant nonlinear intrachannel interactions in strongly dispersion-managed transmission systems', *Opt. Lett.*, 2000, **25**, (24), pp. 1750–1752
4 Liu, X., Wei, X., Gnauck, A.H., Xu, C., and Wickham, L.K.: 'Suppression of interchannel four-wave-mixing-induced ghost pulses in high-speed transmissions by phase inversion between adjacent marker blocks', *Opt. Lett.*, **27**, (13), pp. 1177–1179
5 Xie, C., Kang, I., Gnauck, A.H., Moller, L., Mollenauer, L.F., and Grant, A.R.: 'Suppression of intrachannel nonlinear effects with alternate-polarization formats', *IEEE/OSA J. Lightwave Technol.*, 2004, **22**, (3), pp. 806–812
6 Zweck, J., and Menyuk, C.R.: 'Analysis of four-wave mixing between pulses in high-data-rate quasi-linear subchannel-multiplexed systems', *Opt. Lett.*, 2002, **27**, pp. 1235–1237
7 Moon, J., and Brickner, B.: 'Maximum transition run codes for data storage systems', *IEEE Trans. Mag.*, 1996, **32**, (9), pp. 3992–3994
8 Shapiro, E.G., Fedoruk, M.P., Turitsyn, S.K., and Shafarenko, A.: 'Reduction of nonlinear intrachannel effects by channel asymmetry in transmission lines with strong bit overlapping', *IEEE Photon. Technol. Lett.*, 2003, **15**, (10), pp. 1473–1475
9 Lind, D., and Marcus, B.: 'Symbolic dynamics and coding' (Cambridge University Press, 1995)
10 Agrawal, G.P.: 'Nonlinear fiber optics' (Academic Press, 2001)
11 Cvijetic, M.: 'Optical transmission systems engineering' (Artech House, 2004)
12 Marcus, B., Siegel, P., and Roth, R.: 'An introduction to coding for constrained systems', *in* Huffman, W.C., and Pless, V. (Eds.): 'Handbook of coding theory' (Elsevier Press, 1998)
13 Ait Sab, O.: 'FEC techniques in submarine transmission systems', *Optical Fiber Communication Conf.* (OFC 2001), 2001, **2** pp. TuF1-1–TuF1-3
14 Djordjevic, I., and Vasic, B.: 'Constrained coding techniques for suppression of intrachannel nonlinear effects in high-speed optical transmission', *IEEE/OSA J. Lightwave Technol.*, accepted for publication